Brain Structure and Function (2020) 225:1019–1032
https://doi.org/10.1007/s00429-020-02055-0

ORIGINAL ARTICLE

# Decreased density of cholinergic interneurons in striatal territories in Williams syndrome

**Kari L. Hanson[1,2] · Caroline H. Lew[1] · Branka Hrvoj-Mihic[1] · Deion Cuevas[1] · Demi M. Z. Greiner[1] · Kimberly M. Groeniger[1] · Melissa K. Edler[7] · Eric Halgren[3,4,5] · Ursula Bellugi[6] · Mary Ann Raghanti[7] · Katerina Semendeferi[1,5]**

Received: 16 October 2019 / Accepted: 27 February 2020 / Published online: 18 March 2020


## Abstract

Williams syndrome (WS) is a rare neurodevelopmental disorder caused by the hemideletion of approximately 25–28 genes at 7q11.23. Its unusual social and cognitive phenotype is most strikingly characterized by the disinhibition of social behavior, in addition to reduced global IQ, with a relative sparing of language ability. Hypersociality and increased social approach behavior in WS may represent a unique inability to inhibit responses to specific social stimuli, which is likely associated with abnormalities of frontostriatal circuitry. The striatum is characterized by a diversity of interneuron subtypes, including inhibitory parvalbumin-positive interneurons (PV+) and excitatory cholinergic interneurons (Ch+). Animal model research has identified an important role for these specialized cells in regulating social approach behavior. Previous research in humans identified a depletion of interneuron subtypes associated with neuropsychiatric disorders. Here, we examined the density of PV+ and Ch+ interneurons in the striatum of 13 WS and neurotypical (NT) subjects. We found a significant reduction in the density of Ch+ interneurons in the medial caudate nucleus and nucleus accumbens, important regions receiving cortical afferents from the orbitofrontal and ventromedial prefrontal cortex, and circuitry involved in language and reward systems. No significant difference in the distribution of PV+ interneurons was found. The pattern of decreased Ch+ interneuron densities in WS differs from patterns of interneuron depletion found in other disorders.

**Keywords** Williams syndrome · Interneurons · Basal ganglia · Striatum

## Introduction

Although traditionally best understood with reference to motor function, a growing body of literature has highlighted the importance of basal ganglia structures in cognitive and emotional processes (Grahn et al. 2008, 2009). The striatum comprises the principle input nuclei for the basal ganglia, and receives important overlapping projections from cortical areas that topographically organize its territories into functional loops (Nakano et al. 2000; Haber and Knutson 2010; Choi et al. 2012; Haber 2016). Together, these functional territories form an important site of convergence for integrating information from diverse cortical sources underlying cognitive processes (Morris et al. 2016). The striatum is characterized by the distribution of a variety of inhibitory, GABAergic interneurons, and excitatory, cholinergic interneurons that modulate the function of inputs from regions sharing connectivity with the striatal nuclei and output from striatal medium spiny neurons.

✉ Katerina Semendeferi
ksemende@ucsd.edu

1 Department of Anthropology, University of California San Diego, La Jolla, USA

2 Institute for Neural Computation, University of California San Diego, La Jolla, USA

3 Department of Radiology, University of California San Diego, La Jolla, USA

4 Center for Human Brain Activity Mapping, University of California San Diego, La Jolla, USA

5 Neurosciences Graduate Program, University of California San Diego, La Jolla, USA

6 Salk Institute for Biological Research, La Jolla, CA, USA

7 Department of Anthropology, School of Biomedical Sciences and Brain Health Research Institute, Kent State University, Kent, USA

These diverse populations of inhibitory interneurons express calbindin, calretinin, parvalbumin, somatostatin, neuropeptide Y, and NADPH-diaphorase, and combined, constitute around 20% of total striatal neuron populations in the neurotypical human brain (Wu and Parent 2000; Bernácer et al. 2012; Lecumberri et al. 2018). Among these, fast-spiking interneurons express the calcium-binding protein parvalbumin (PV+) and forms multiple synapses with single cortical afferents in the striatum (Koós and Tepper 1999; Tepper et al. 2010; Berke 2011).

Striatal cholinergic interneurons (Ch+) are excitatory neurons that comprise less than 1% of total neuron populations in the human striatum (Bernacer et al. 2007, 2012; Stephenson et al. 2017). Despite their sparse distribution, these extremely large, heavily branched neurons share extensive connections with cortical and subcortical projections, and modulate inputs to local inhibitory interneurons and medium spiny projection neurons within the striatum (Bolam et al. 1984; Contant et al. 1996; Pakhotin and Bracci 2007). Data produced from rodent models support the hypothesis that Ch+ interneurons contribute to the modulation of social behavior. Martos and colleagues (2017) showed that selective ablation of Ch+ interneurons led to a significant increase in compulsive, socially directed (not object-focused) exploratory behavior in mice. Rapanelli and colleagues (2017) additionally demonstrated that the ablation of both Ch+ and fast-spiking PV+ in the caudate and putamen may result in 'autistic' behaviors, including repetitive and stereotyped behavior and reduced social interaction, particularly in male (but not female) mice. Importantly, the behavioral pattern was observed only when both types of neurons were targeted. These deficits may relate to the relationship between interneurons and medium spiny projecting neurons in the striatum. Together, these findings suggest that Ch+ and PV+ interneurons contribute to a mechanism that may selectively regulate socially directed behavior.

Williams syndrome (WS) is a rare genetic disorder with an unusual cognitive phenotype characterized most saliently by the profound disinhibition of social behavior (Järvinen-Pasley et al. 2008; Järvinen et al. 2013). Individuals with WS are known to have an unusually high drive to engage in social interactions, which may be attributed to a deficit in the inhibitory control of social behavior (Little et al. 2013) and dysfunction of behavioral response inhibition (Mobbs et al. 2007). Further evidence for pathology of striatal morphology and its contribution to functional deficits come from structural imaging, where decreases in gray matter volume in the caudate, as well as decreased volume of the putamen and nucleus accumbens have been reported (Reiss et al. 2000, 2004; Fan et al. 2017). Taken together, these findings suggest that the unique cognitive profile in WS may be associated with abnormalities of frontostriatal circuitry.

Imbalances of inhibitory and excitatory neuronal activity, both in the cerebral cortex as well as in subcortical structures, are thought to contribute to dysfunction in a variety of psychiatric and neurodevelopmental disorders (Yizhar et al. 2011; Marín 2012), including autism (Gogolla et al. 2009; Zikopoulos and Barbas 2013; Nelson and Valakh 2015; Hashemi et al. 2017). Our preliminary findings in WS (Hanson et al. 2018a) suggested a percentwise decrease in the density of Ch+ interneurons in the caudate. Here, we examined the density of Ch+, as well as PV+, interneurons in the striatum in an expanded sample of neurotypical subjects (NT) and subjects with WS. Our aim was to determine if there are differences in the density of Ch+ and PV+ interneurons between NT subjects and subjects with WS within striatal territories with shared connectivity with the prefrontal cortex (PFC), and how the pattern of their distribution may relate to differences observed in other neuropsychiatric disorders. Given the unusual social phenotype observed in WS, it was expected that altered Ch+ and PV+ interneuron densities may contribute to deficits in behavioral inhibition observed in WS, due to these cell types' putative role in modulating social approach behavior.

## Methods

### Materials

Table 1 lists information on all subjects from whom postmortem materials were used in the current study. All brain tissue samples were collected from donors for whom an informed consent for brain autopsy and use of clinical data and demographic information for research was obtained. The brains of seven subjects with behaviorally confirmed diagnoses of WS (four males and three females, average age $38.5 \pm 7.3$ years) in the Ursula Bellugi Williams Syndrome Brain Collection were included in the sample. Genetic confirmation of WS, based on *FISH* for elastin, was confirmed for five out of seven subjects. Medical history for two subjects, for whom genetic deletion data were not available (WS1 and WS13) indicated key phenotypic traits, including distinctive facies and significant history of supravalvular aortic stenosis (SVAS), consistent with the genetic disorder's biomedical profile (Morris and Mervis 2000; Pober 2010). Six NT subjects (four males and two females, average age $39.0 \pm 6.3$ years) were provided in collaboration with the University of Maryland Brain and Tissue Bank, who granted ethical permission for use of postmortem materials in this research. All brain samples were cryosectioned at 40 µm and a 1-in-10 series stained with 0.25% thionine solution for Nissl. Independent sample t tests revealed no significant difference in age ($t_{11} = 0.05$, $p = 0.96$), postmortem

**Table 1** Subject background information

| Subject | Age at death (years) | Sex | Diagnosis | PMI (hours) | Cause of death |
|---|---|---|---|---|---|
| WS 10 | 18 | M | WS | 24 | WS/cardiac complications |
| 4916 | 19 | M | NT | 5 | Drowning |
| WS 15 | 25 | F | WS | 24 | WS/cardiac complications |
| 5350 | 25 | F | NT | 26 | Sepsis |
| WS 1 | 31 | M | WS | 26 | WS/cardiac complications |
| 5614 | 31 | M | NT | 24 | Acute drug intoxication |
| WS 14 | 42 | F | WS | 12 | WS/cardiac complications |
| WS 9 | 43 | F | WS | 12 | WS/cardiac complications |
| 5445 | 42 | F | NT | 10 | Pulmonary thromboembolism |
| WS 12 | 45 | M | WS | 24 | WS/cardiac complications |
| 5875 | 45 | M | NT | 19 | Aortic dissection |
| WS 13 | 69 | M | WS | 8 | WS/cardiac complications |
| 5943 | 69 | M | NT | 23 | Acute coronary artery thrombosis |

*PMI* postmortem interval

interval ($t_{11}=0.16$, $p=0.87$), or fixation duration ($t_{11}=0.04$, $p=0.97$) between WS and NT subjects.

## Immunohistochemical staining

Two 1-in-20 series of sections were selected from the interval spanning the rostral striatum and head of the caudate nucleus rostral to the emergence of the anterior commissure in the coronal plane for each individual for immunohistochemistry. Prior to immunohistochemical processing, sections were stored at − 20 °C in cryoprotective solution. Sections were stained for choline acetyltransferase (ChAT) and parvalbumin using an avidin–biotin peroxidase method previously described (Raghanti et al. 2008) and developed for optimal use in archival fixed tissues. Briefly, floating tissue sections were rinsed in PBS for 50 min, and pre-treated for antigen retrieval utilizing a 0.05% citraconic acid solution at 86 °C for 30 min. Endogenous peroxidases were quenched by incubation in a methanol and hydrogen peroxide solution. Sections were pre-blocked in a solution of normal sera and Triton-X detergent prior to incubation primary antibodies for ChAT and PV.

## Cholinergic interneurons

Free-floating tissue sections were incubated in an anti-ChAT polyclonal antibody raised in goat (Millipore AB-144P) at a 1:500 dilution concentration, continuously shaken for 24 h at room temperature, followed by 24 h at 4 °C. The primary antibody selected labels a band at approximately 68 kDa in humans and nonhuman primates, and has been validated for immunohistochemical use in both nonhuman primate (Raghanti et al. 2008; Stephenson et al. 2017) and human (Bernácer et al. 2007; Raghanti et al. 2008; Stephenson et al. 2017) tissue.

## Parvalbumin

Adjacent 1-in-20 series of free-floating tissue sections from each subject were incubated in a monoclonal antibody raised against parvalbumin (Swant #235) at a 1:5000 dilution concentration, and continuously shaken for 24 h at room temperature followed by 24 h at 4 °C. The primary antibody specifically stains the $^{45}$Ca-binding site of parvalbumin, and has been extensively validated for use in human and nonhuman primate fixed tissue (Prensa et al. 1999; Sherwood et al. 2009).

Following incubation in primary antibody, all sections were rinsed and incubated in a biotinylated secondary antibody (dilution 1:200), followed by an avidin–peroxidase complex (ABC kit; PK-6100, Vector Laboratories, Burlingame, CA). A 3,3′-diaminobenzidine chromogen with nickel enhancement (SK-4100, Vector Laboratories) was utilized to visualize immunoreactive cells and fibers with robust staining of cell bodies and their processes (Figs. 1 and 2). Stained sections were mounted on gelatin-coated slides that were blinded to the investigator for diagnosis prior to quantification. No qualitative differences in staining or in the distribution of positively stained cells were observable between NT and WS subjects that would distinguish them during counting procedures.

## Regions of interest

Boundaries for five territories, including the dorsal and medial territories of the caudate nucleus, the nucleus accumbens region, and the medial associative and dorsal

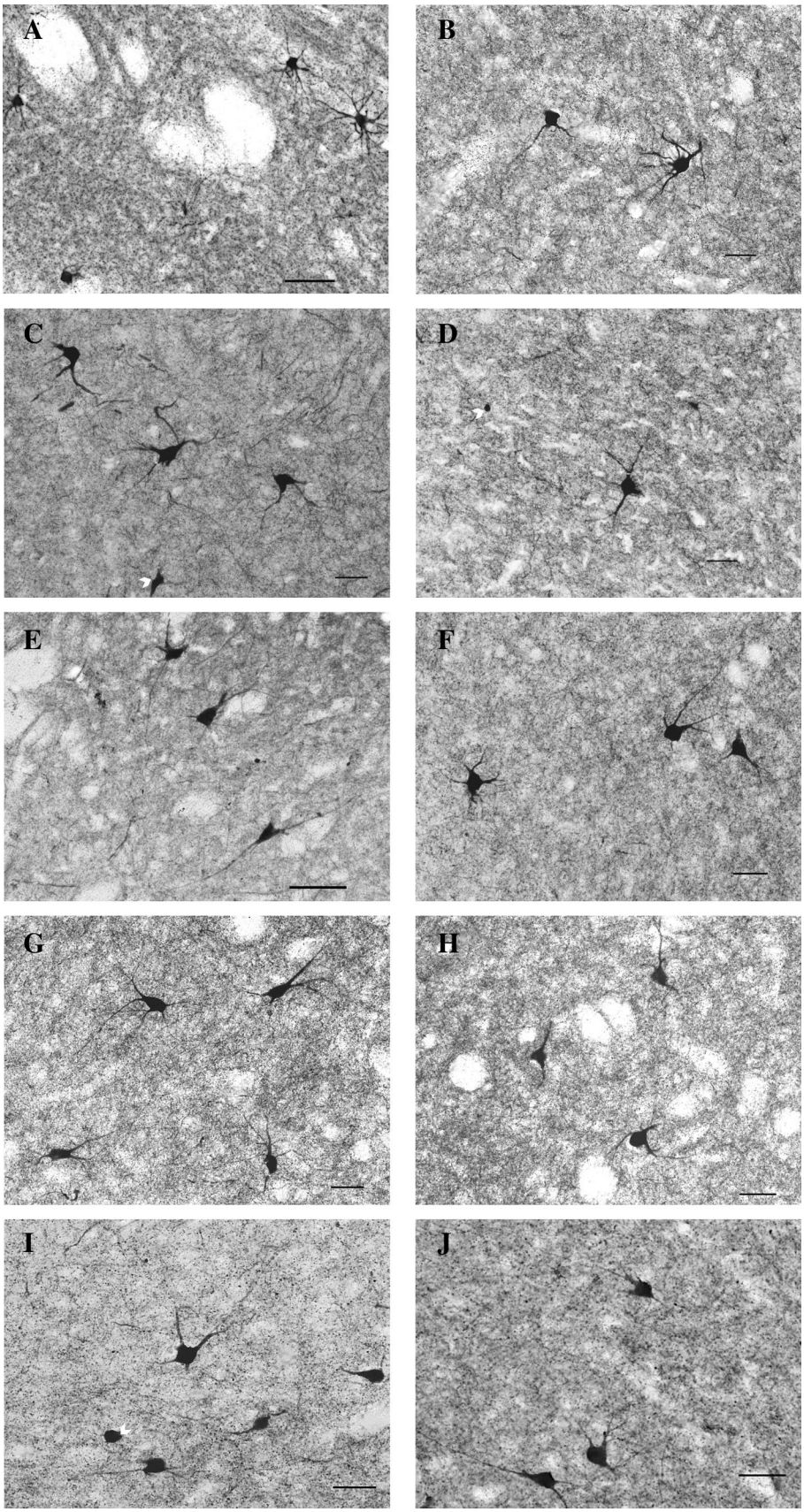


**Fig. 1** Examples of neurons and fibers positively stained for ChAT+ in NT (left) and WS (right) subjects in five striatal regions of interest including the dorsal (**a**, **b**) and medial (**c**, **d**) caudate, dorsal (**e**, **f**) and medial (**g**, **h**) putamen, and nucleus accumbens (**i**, **j**) regions. Arrows denote incomplete cell bodies of neurons that did not meet inclusion criteria. Scale bar = 50 um

associative-sensorimotor regions of the putamen were established from adjacent series of Nissl-stained sections as previously described (Hanson et al. 2018a, b; Fig. 3). Care was taken to sample within these territories consistently, avoiding transitional areas and the fibers of the internal capsule. Due to their highly sparse distribution and consistent with previous observations (Kataoka et al. 2010), PV+ interneuron density could not be reliably quantified in the nucleus accumbens region, and was, therefore, not measured.

### Stereological quantification

Quantitative analyses were performed by computer-assisted stereology using a Dell workstation receiving live video feed from an Optronics MicroFire color video camera (East Muskogee, OK) attached to a Nikon 80i light microscope, equipped with a Ludl MAC5000 motorized stage and a Heidenhain *z*-axis encoder. The optical dissector probe was used in conjunction with fractionator sampling using StereoInvestigator software (v. 10, MBF Bioscience, Williston, VT). Regions of interest were traced at 4× magnification (N.A. 0.75), and a square grid no larger than 1,000 μm$^2$ was superimposed in random orientation over the region of interest. Six sections per subject spanning the rostrocaudal extent of the head of the caudate nucleus, putamen, and nucleus accumbens regions (800 μm apart) were sampled for density of Ch+ and PV+ interneurons. Interneurons were counted at 20× magnification (N.A. 0.75) in a 350 μm$^2$ counting frame with a dissector height of 9 μm, with a coefficient of error (Gundersen $m = 1$) less than or equal to 0.1. Interneurons were counted only if they had a well-defined, darkly stained soma that came into view within the counting frame and initial segments of at least one visibly stained process. Incomplete neurons were excluded and comprised only a small proportion of stained neurons (typically less than 2 in approximately 20–25 sampling sites per section). Soma area for interneurons was additionally measured in one in every five interneurons counted using the Nucleator probe with a 4-point array in StereoInvestigator. Total density of interneurons was calculated as the estimated population divided by the planimetric volume of the region sampled. We additionally compared the density of Ch+ and PV+ interneurons relative to the total density of neurons for all regions of interest, as previously determined from Nissl-stained sections and quantified using previously published parameters (Hanson et al. 2018a, b) in the newly sampled subjects and territories. Additional stereological parameters, including average number of sampling sites and coefficient of error by region of interest, are listed in Tables 2 and 3.

### Statistical analyses

All statistical analyses were performed using GraphPad Prism (Version 7, La Jolla, CA). Two-way ANOVAs were calculated ($\alpha < 0.05$) to compare the density of Ch+ and PV+ interneurons with region of interest and condition (WS v. NT) as independent variables. All data were subject to Grubb's test (GraphPad test for outliers) to determine if any single value represented a significant outlier from others by diagnostic category (WS or NT), but no outliers were detected. The percent of Ch+ and PV+ interneurons relative to the total density of neurons was additionally compared across all regions. Mann–Whitney *U* tests were utilized as post hoc tests to compare values for interneuron densities, percentages, and soma area in each region of interest between WS and NT subjects.

## Results

Results for the density of Ch+ and PV+ interneurons in all five areas are summarized in Figs. 4 and 5. Table 4 summarizes average interneuron densities and the percentage of total neurons these account for in all areas. For Ch+ interneurons, ANOVAs revealed significant effects of region of interest ($F_{4,53} = 6.75$, $p = 0.0002$) and diagnosis ($F_{1,53} = 12.89$, $p = 0.0007$), though no interaction between diagnosis and region of interest was observed ($F_{4,53} = 0.69$, $p = 0.60$). A significant effect of region of interest was observed for PV+ interneuron density ($F_{3,37} = 3.36$, $p = 0.03$), but no significant effect of diagnosis ($F_{1,37} = 1.50$, $p = 0.23$) or interaction between diagnosis and region of interest ($F_{3,37} = 1.43$, $p = 0.25$) was found. The percent of Ch+ neurons as a proportion of total neurons showed no significant interaction between region of interest or diagnosis ($F_{4,53} = 0.64$, $p = 0.63$), but significant effects of region of interest ($F_{4,53} = 4.94$, $p = 0.002$) and diagnosis ($F_{1,53} = 5.05$, $p = 0.03$) were observed. The percent of PV+ interneurons as a proportion of total neurons showed no significant interaction between region of interest and diagnosis ($F_{3,43} = 0.33$, $p = 0.84$), and no significant effect of diagnosis ($F_{1,43} = 0.19$, $p = 0.66$), but a significant effect of region of interest ($F_{3,43} = 3.61$, $p = 0.02$) was observed.

### Dorsal caudate

The highest average values for Ch+ density in the caudate were found in the dorsal portion. No difference in the density of Ch+ interneurons (mean ± SEM) was observed between WS (175 ± 22.2/mm$^3$) and NT (194 ± 22.5/mm$^3$) subjects (Mann–Whitney *U* test, $p = 0.53$). Soma area for Ch+ interneurons also did not differ significantly (837 ± 58.5 μm$^2$ WS vs. 801 ± 52.8 μm$^2$ NT, $p = 0.55$).

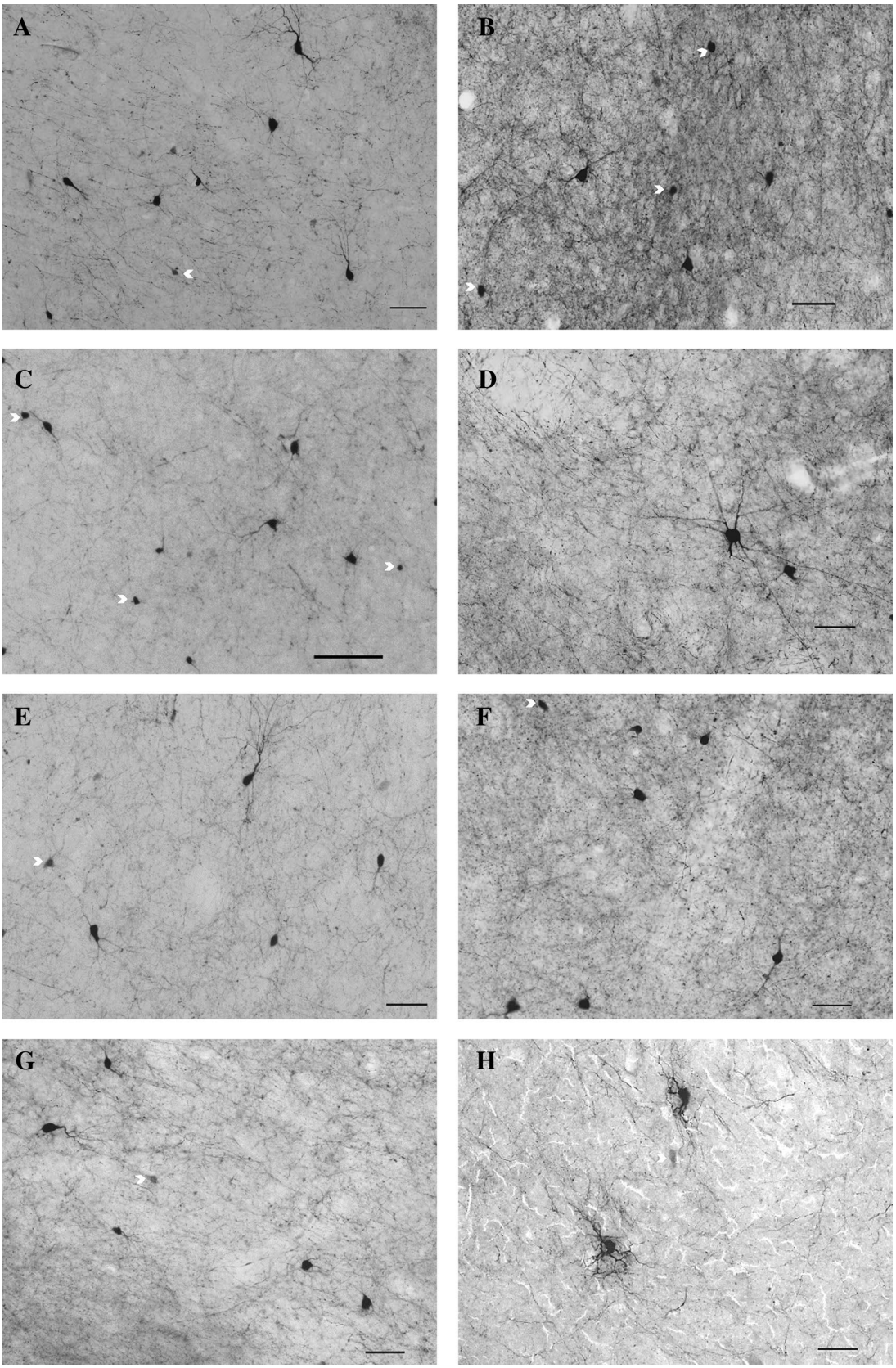
A
B
C
D
E
F
G
H

◂**Fig. 2** Examples of neurons and fibers positively stained for PV in NT (left) and WS (right) subjects in four striatal regions of interest including the dorsal (**a**, **b**) and medial (**c**, **d**) caudate, dorsal (**e**, **f**) and medial (**g**, **h**) putamen regions. Arrows denote incomplete cell bodies of neurons that did not meet inclusion criteria. Scale bar = 50 um

No significant difference was observed in PV+ interneuron density (209 ± 20.1/mm$^3$ WS vs. 294 ± 47.3/mm$^3$ NT, $p = 0.23$) or soma area (283 ± 13.5/mm$^3$ WS vs. 286 ± 12.7/mm$^3$ NT, $p = 0.85$). No difference in the percent of total neurons comprised by PV+ (1.02% WS vs. 1.06% NT, $p = 0.95$) or Ch+ (0.78% WS vs. 0.82% NT, $p = 0.84$) neurons was observed in this region.

### Medial caudate

A significant decrease in the density of Ch+ interneurons was observed in the medial caudate nucleus of WS individuals compared to NT (108 ± 10.3/mm$^3$ in WS vs. 176 ± 21.0/mm$^3$ NT; $p = 0.0082$). Average Ch+ soma area did not differ significantly between NT (731 ± 78.2 μm$^2$) and WS (768 ± 57.0 μm$^2$, $p = 0.84$). No significant difference in the density (153 ± 20.3/mm$^3$ WS vs 190 ± 36.1/mm$^3$, $p = 0.63$) or soma area (276 ± 11.1 μm$^2$ in WS vs. 287 ± 18.9 μm$^2$ NT; $p = 0.66$) of PV+ interneurons was observed. A significant decrease in the percent of total neurons comprised by Ch+ neurons was observed (0.41% WS vs. 0.67% NT, $p = 0.01$), but no significant difference was observed in percent of PV+ interneurons (0.65% WS vs. 0.78% NT, $p = 0.63$).

### Dorsal putamen

Greater average density of Ch+ interneurons was observed in the dorsal territory of the putamen as compared to its medial territories. No significant difference in the distribution of PV+ (159 ± 19.7 NT vs. 169.4 ± 21.4 WS, $p = 0.63$) or Ch+ (262 ± 37.8 NT vs. 204 ± 24.7, $p = 0.24$) interneurons or soma area was observed between NT and WS. No difference was observed in total soma area for Ch+ (722 ± 32.0 WS vs. 754 ± 21.7 NT, $p = 0.59$) or PV+ (338 ± 7.1 WS vs. 312 ± 8.2 NT, $p = 0.23$) neurons. Percent of total neurons represented by Ch+ (0.66% WS vs. 1.04% NT, $p = 0.72$) and PV+ (0.67% WS vs. 0.66% NT, $p = 0.63$) was not significantly different.

### Medial putamen

The lowest density of Ch+ interneurons in NT subjects was observed in the associative region of the medial putamen, consistent with previously reported average values for its precommissural territories (Bernácer et al. 2007). Average values for Ch+ interneuron density did not differ significantly between NT and WS subjects (158 ± 20.6/mm$^3$ NT vs. 136 ± 16.2/mm$^3$ WS, $p = 0.54$). Though average density for PV+ interneurons was 27.3% lower in WS as compared to NT subjects, this difference was not statistically significant (146 ± 5.3/mm$^3$ WS vs. 195 ± 30.6/mm$^3$, $p = 0.0513$), nor did they comprise a smaller percentage of total neurons (0.62% WS vs. 0.68% NT, $p = 0.95$). No significant difference in soma area was observed for PV+ (302 ± 11.0 μm$^2$ WS vs. 320 ± 2.4 μm$^2$, $p = 0.40$) or Ch+ neurons (746 ± 76.3 μm$^2$ NT vs. 751 ± 61.4 μm$^2$ WS; $p = 0.90$) in this region.

### Nucleus accumbens

Average density of Ch+ interneurons was significantly lower in WS subjects (167 ± 12.6/mm$^3$ WS vs. 230 ± 22.2 NT, $p = 0.04$), as was the percent of total neurons staining positive for Ch+ (0.53% WS vs. 0.72% NT, $p = 0.01$). Ch+ soma area did not differ significantly in WS (757 ± 57.1 μm$^2$) as compared to NT subjects (686 ± 51.6 μm$^2$, $p = 0.3859$). PV+ interneurons were not quantified in the NA region due to their sparse distribution.

## Discussion

In the present work, our aim was to analyze the density of Ch+ and PV+ interneurons in the rostral territories of the striatum in WS as compared to NT subjects. The regions of interest examined here comprise a significant portion of the striatum rostral to the anterior commissure, and were targeted for their connectivity with several areas of the PFC: orbitofrontal (BAs 11, 13, 14, and 12), anterior cingulate and ventromedial (BAs 24b, 25, and 32) and dorsal (BA 9/46) areas of the PFC (Haber 2003; Haber et al. 2006; Haber and Knutson 2010). Ch+ interneuron densities in NT subjects for all regions of interest reported here lie within the range of variation previously reported for neurotypical subjects for the regions of interest (Bernácer et al. 2007; Kataoka et al. 2010). Values for PV+ interneuron density in NT subjects also fell within the range of variation previously reported (Kataoka et al. 2010; Bernácer et al. 2012; Lecumberri et al. 2018). In WS, we found a significant reduction in the density of Ch+ interneurons in the medial caudate nucleus and nucleus accumbens, and no difference compared to NT for PV+.

These findings add to a growing body of literature that point to significant changes in WS in structures guiding social responses and inhibitory behavioral control, suggesting that the circuits critically involved in these behaviors may be compromised. Our previous analyses (Hanson et al. 2018b) have indicated that the caudate nucleus in WS is characterized by an excess of glia, and particularly

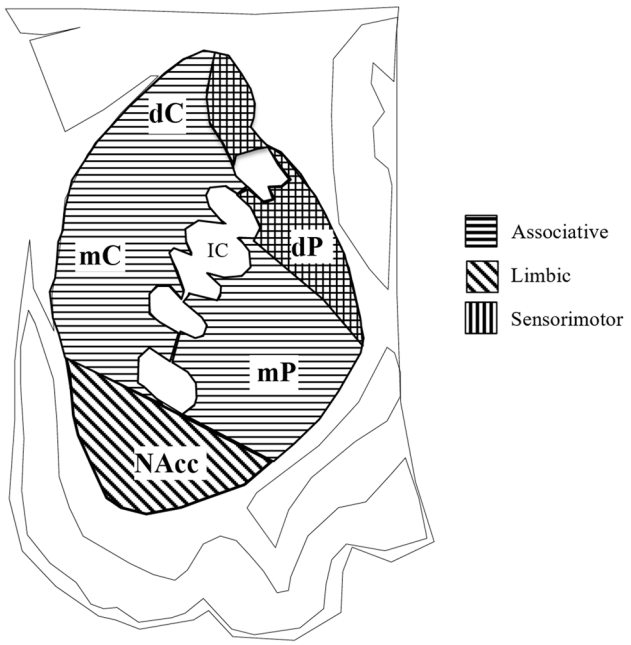


**Fig. 3** Regions of interest sampled corresponding to the dorsal (dC) and medial (mC) caudate nucleus, medial putamen (mP), dorsal putamen (dP), and nucleus accumbens (NA) regions. Dorsal regions of the putamen and dorsomedial regions of the caudate receive overlapping sensorimotor and associative projections. Adapted from Bernácer et al. (2007); Haber and Knutson (2010); Averbeck et al. (2014)

oligodendrocytes, which may relate to local differences in connectivity with specific areas of the PFC. These findings are particularly interesting given previous reports (Lew et al. 2017) of a decrease in neuron density in the orbital PFC of WS individuals (specifically, BA 11, which projects to the mC) that was not observed in primary somatosensory, motor, or visual cortex (BAs 3, 4, and 18). This area, as well as BA 10, also displayed an altered pattern of dendritic complexity in pyramidal neurons as compared to NT subjects (Hrvoj-Mihic et al. 2017). Additionally, BA 25 of the ventromedial PFC, which projects to the most ventral territories of the medial caudate and nucleus accumbens, showed decreased neuronal density in infragranular layers, and a substantially greater density of glia in WS (Wilder et al. 2018). These key regions of the PFC form important connections with the striatum at the specific sites where we observed decreased Ch+ neuron density, supporting the assertion that frontostriatal systems are particularly affected in the WS neuroanatomical phenotype.

Our observations in the striatum of individuals with WS can be considered in the context of other neuropsychiatric disorders where striatal interneurons are found to be decreased in density (Table 5). A decrease in Ch+ interneuron density has been observed in schizophrenia, which is characterized by disruptions in emotional regulation, deficits in reward prediction, and generalized anhedonia, attributed in part to abnormalities of the midbrain dopaminergic system affecting innervation of the basal ganglia (Perez-Costas et al. 2010). The decrease is most notable in the ventral striatum, inclusive of the most ventral territories of the caudate and nucleus accumbens regions (Holt et al. 1997, 2005). These areas are also affected in our WS sample. Depletion of Ch+ is found in Tourette syndrome (TS), a disorder characterized by the persistence of multiple involuntary motor and vocal tics. In TS, this depletion is found primarily in associative and sensorimotor territories of the dorsal striatum (Kataoka et al. 2010). By contrast, we found a decrease of Ch+ interneurons specific to the medial caudate nucleus in WS, with no significant differences observed in other territories. Specific deficits of Ch+ interneurons were noted in early immunohistochemical studies (Selden et al. 1994a) of Alzheimer's disease (AD) in the ventral striatum, where a dramatic (> 70%) decrease in numbers was observed in a two-dimensional study of sections stained for acetylcholinesterase. Nevertheless, given recent advances in the study and complexities of the disease, the significance of these findings to contemporary insights of AD is complex (see Craig et al. 2011; Nava-Mesa et al. 2014; Sanabria-Castro

**Table 2** Stereological sampling parameters for Ch+ interneurons

| Region of interest | Diagnosis | Mean no. sampling sites | Mean no. neurons counted | Mean CE value (Gundersen $m = 1$) |
|---|---|---|---|---|
| dC | WS | 256 | 117 | 0.10 |
| | NT | 238 | 108 | 0.09 |
| mC | WS | 430 | 125 | 0.10 |
| | NT | 324 | 154 | 0.09 |
| dP | WS | 274 | 100 | 0.10 |
| | NT | 215 | 95 | 0.10 |
| mP | WS | 321 | 116 | 0.09 |
| | NT | 286 | 124 | 0.10 |
| NAcc | WS | 211 | 86 | 0.10 |
| | NT | 227 | 146 | 0.09 |

**Table 3** Stereological sampling parameters for PV+ interneurons

| Region of interest | Diagnosis | Mean no. sampling sites | Mean no. Neurons counted | Mean CE value (Gundersen $m=1$) |
|---|---|---|---|---|
| dC | WS | 223 | 139 | 0.09 |
| | NT | 293 | 153 | 0.09 |
| mC | WS | 225 | 107 | 0.09 |
| | NT | 330 | 167 | 0.10 |
| mP | WS | 279 | 141 | 0.09 |
| | NT | 235 | 121 | 0.09 |
| dP | WS | 219 | 100 | 0.10 |
| | NT | 249 | 81 | 0.10 |

et al. 2017 for review). Ch+ interneurons seem to be differentially affected in the limbic territories in the striatum in AD, which may relate to the high density of neurofibrillary tangles observed in the nucleus accumbens (Selden et al. 1994b) but not in the head of the caudate nucleus.

Data for striatal PV+ interneuron densities do not exist in the literature for autism spectrum disorder (ASD), but a reduced density of small, calretinin-positive (CR) interneurons was found in the caudate nucleus in ASD as compared to neurotypical subjects (Adorjan et al. 2017). CR+ neurons comprise the most predominant cell type in the striatum in primates, and display a range of morphotypes with diverse properties (Wu and Parent 2000). Approximately 90% of the large CR+ interneurons in the striatum are cholinergic interneurons, but these large neurons did not show a similar pattern of reduced density in ASD subjects examined. Reduction of small GABAergic CR+ interneurons may relate to variants observed in the gene *CNTNAP2* in ASD, which was associated with decreased CR+ neurons in the cerebral cortex in an animal model (Peñagarikano et al. 2011). One postmortem study has additionally confirmed that CR+ neurons are reduced in number in BA 9 in ASD (Hashemi et al. 2017). *CNTNAP2* is not a part of the deletion observed in WS, and its variation in ASD may identify a subset of cases within this heterogeneous disorder with diverse genetic etiology. Nevertheless, calretinin-positive neurons may represent a further site of altered neuronal distribution in WS and provide a future direction for ongoing research into inhibitory systems in the disorder.

The medial caudate corresponds to territories that form networks important for decision-making, motivation, and reward (Haber and Behrens 2014). This region is additionally important for language function and vocalizations, and corresponds to territories where humans with dysfunctional *FOXP2* genes display hyperactivation relative to NT participants in fMRI and PET language tasks (Vargha-Khadem et al. 1998; Liégeois et al. 2003). Although language function in WS is typically referred to as preserved relative to other cognitive faculties, such as visuospatial cognition (Nakamura et al. 2001; Farran and Jarrold 2003; Atkinson et al. 2003, 2007; Meyer-Lindenberg et al. 2004), global

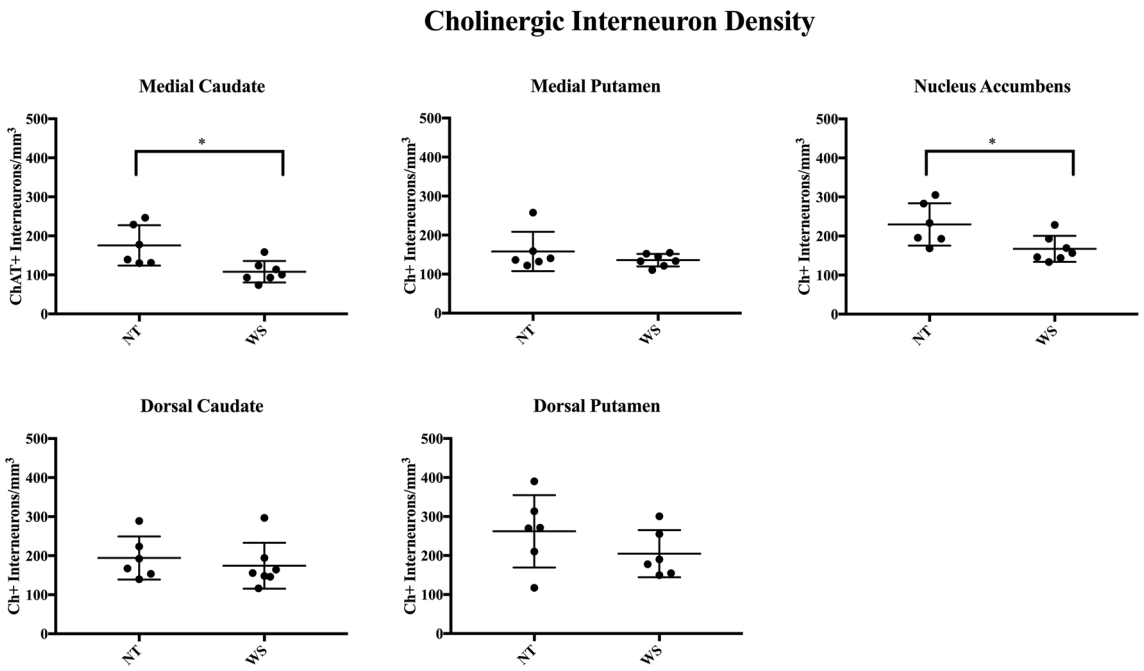


**Fig. 4** Results of stereological analyses for Ch+ interneuron density. A significantly lower density of Ch+ interneurons was found in the medial caudate (mC) and nucleus accumbens (NAcc) regions, but not in the putamen

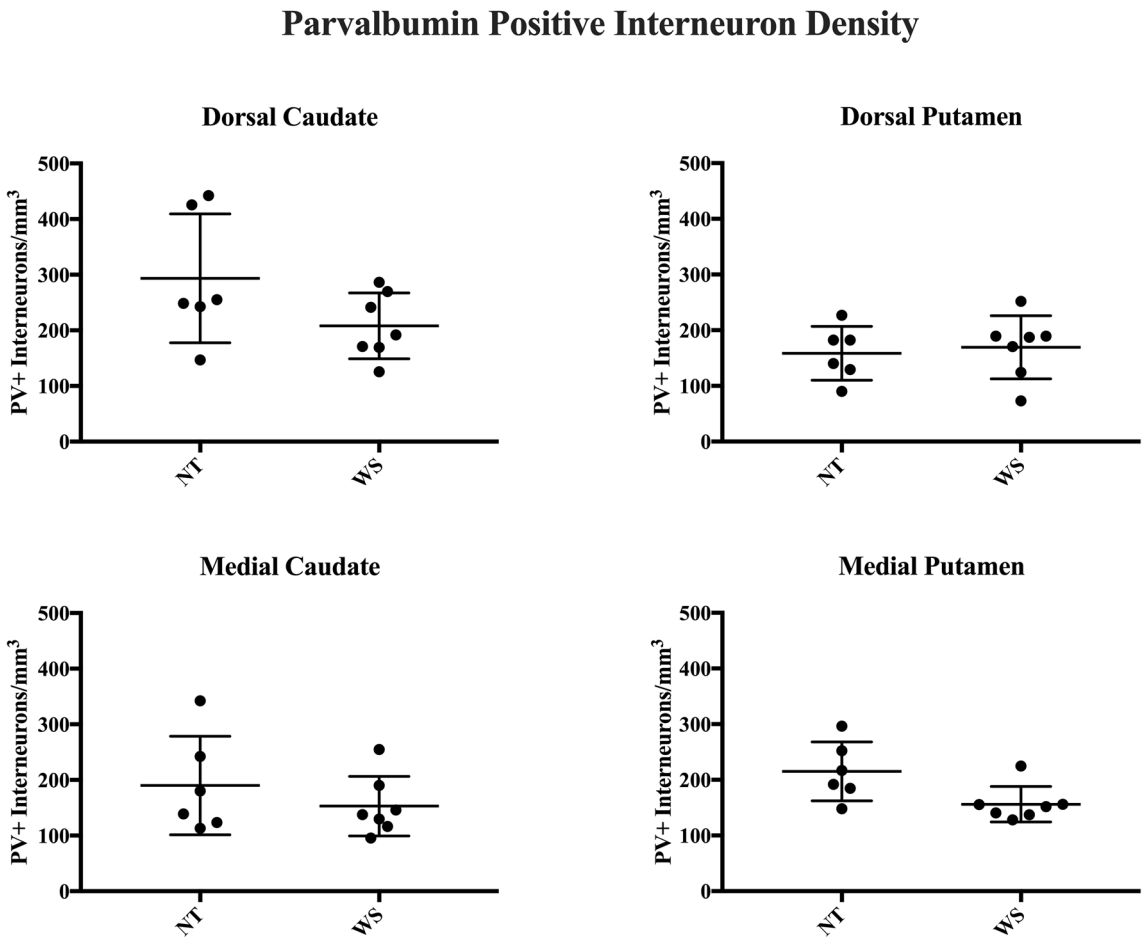


**Fig. 5** Results of stereological analyses for PV+interneuron density. No significant difference in the density of PV+interneurons was observed between WS and NT subjects

**Table 4** Mean density of interneurons sampled and percent of total neurons by region of interest

| | Dorsal caudate | Medial caudate | Dorsal putamen | Medial putamen | Nucleus accumbens |
|---|---|---|---|---|---|
| NT Ch+density % total neuron density | 194 ± 22.5<br>0.82% | 176 ± 21.0<br>0.67% | 262 ± 37.8<br>1.04% | 158 ± 20.6<br>0.51% | 230 ± 22.2<br>0.72% |
| WS Ch+density % total neuron density | 175 ± 22.2<br>0.78% | 108 ± 10.3<br>0.41% | 204 ± 24.7<br>0.66% | 136 ± 16.2<br>0.53% | 167 ± 12.6<br>0.53% |
| % Difference in Ch+ | − 11.64% | − 51.58%* | − 0.22% | + 0.01% | − 40.13%* |
| NT PV density % total neuron density | 294 ± 47.3<br>1.06% | 190 ± 36.1<br>0.78% | 159 ± 19.7<br>0.66% | 195 ± 30.6<br>0.68% | Not measured |
| WS PV+density % total neuron density | 209 ± 20.1<br>1.02% | 153 ± 20.3<br>0.65% | 169 ± 21.4<br>0.67% | 146 ± 5.3<br>0.62% | Not measured |
| % Difference in PV+ | − 33.74% | − 31.8% | + 0.07% | − 27.3% | Not measured |

* indicates a significant decrease in density

IQ (Searcy et al. 2004), and working memory (Morris and Mervis 2000; Robinson et al. 2003; Sampaio et al. 2008, 2010), select abnormalities of language use and function are observed in the disorder, including deficiencies in syntax, phonology, and lexical semantics (Brock 2007) as well as spatial and temporal elements of language (Karmiloff-Smith et al. 1997; Phillips et al. 2004). Additional study of neurotransmitter innervation may be of particular interest for understanding these language deficits in WS, given the role the putamen may play (Booth et al. 2007; Balsters et al.

**Table 5** Summary of evidence for aberrant striatal interneuron distribution in selected neurological disorders in humans

| Disorder | Key finding | Citation |
|---|---|---|
| Williams syndrome (WS) | Decreased density of ChAT+ neurons in medial caudate and accumbens (IHC; postmortem stereological study) | Present study |
| Autism spectrum disorders (ASD) | Decreased density of small CR+ neurons in caudate | Adorjan et al. (2017) |
| Schizophrenia | Reduced density of Ch+ interneurons in medial caudate, ventral striatum | Holt et al. (1997, 2005) |
| Tourette's syndrome (TS) | Reduced density of striatal PV+ and Ch+ interneurons in associative/sensorimotor territories of dorsal striatum | Kalanithi et al. (2005), Kataoka et al. (2010) |
| Alzheimer's disease (AD) | Decreased density of Ch+ neurons in ventral striatum (by area) | Lehéricy et al. (1989), Selden et al. (1994a) |

2017; Viñas-Guasch and Wu 2017) in language processing and production. Though no significant difference was observed in the total density of PV+ interneurons, previous research (Fan et al. 2017) has suggested that gross differences in putamen volume may contribute to the disorder's distinctive phenotype.

In addition to language functions, the medial caudate may be particularly important for social interaction and language, and has been the site of important neuroanatomical changes during human evolution (Raghanti et al. 2008). While the whole striatum has undergone a substantial reduction in relative size in the human brain in recent primate evolution (Barger et al. 2014), significant increases in dopaminergic innervation of the medial caudate have been observed in humans as compared to anthropoid primates, including apes (Raghanti et al. 2016). While cholinergic innervation did not differ across taxa in the medial caudate, humans and apes display a significant predominance of multipolar Ch+ as compared to unipolar and bipolar morphotypes, which displayed a higher frequency in monkeys (Stephenson et al. 2017). Though basal ganglia components are frequently regarded as being highly conserved, these differences may indicate enhanced synaptic plasticity and neurotransmission, which may relate to the evolution of language and reward systems.

Patterns of morphological differences in ASD serve as an interesting counterpoint to those observed in WS, particularly in their contrasting behavioral phenotypes and genetic profiles. Duplications in the deleted region in WS have been shown to result in a canonically autistic behavioral phenotype characterized by language delays and reduced social behavior (Berg et al. 2007; Velleman and Mervis 2011; Sanders et al. 2012), suggesting disparate effects of the gene deletion or duplication in WS and ASD respectively, with implications for the underlying neuroanatomy. Structural imaging studies have revealed increased caudate volume (Sears et al. 1999; Langen et al. 2007) and early overgrowth of the caudate in ASD (Langen et al. 2012), which is strongly associated with repetitive behaviors in the disorder (Estes et al. 2011) and not commonly observed in WS (Rodgers et al. 2012). Decreased frontostriatal connectivity in the caudate nucleus has also been observed (Di Martino et al. 2011) in ASD, and functional imaging studies have noted reduced frontostriatal activation (Shafritz et al. 2008), as well as aberrant processing of reward and reduced connectivity in the nucleus accumbens (Delmonte et al. 2013), particularly related to social stimuli (Kohls et al. 2013). Whereas reduced neuron density is observed in the caudate and nucleus accumbens in ASD (Wegiel et al. 2014), no differences in total neuron density were observed in these structures in WS, but an excess of glia, and particularly oligodendrocytes, was found (Hanson et al. 2018b) in the caudate, suggesting abnormalities of cellular distribution that may contribute to frontostriatal dysfunction. Additionally, an increase in the number of neurons in the lateral nucleus of the amygdala has been observed in WS (Lew et al. 2018), whereas this region showed evidence for a decrease in neuron number in ASD (Schumann and Amaral 2006). The amygdala also demonstrates a disparate pattern of serotonergic innervation in WS and ASD, including an increased density of serotonergic axons in ASD and a reduced density in WS as compared to NT individuals (Lew et al. 2020). In light of these contrasting patterns in microstructure, additional perturbations of neural circuitry may be seen in the striatum in ASD cases.

## Conclusion

The present study targeted PV+ and Ch+ interneurons in territories of the striatum in WS due to their putative role in social approach behavior. In WS, we found a significant decrease in cholinergic interneuron density in the medial caudate nucleus that likely contributes to the reduced inhibitory control of social behavior, in a specific territory of the striatum targeted for its role in social cognition. Multiple neurological disorders involve perturbations of interneuronal circuitry, which is likely important for social behavior, emotional regulation, and behavioral control. Decreases in interneuron density in neurological disorders follow

distinctive patterns that seem to relate to shared connectivity with cortical regions and modulation of cortical afferents. The topographical organization of the striatum, and particularly the caudate nucleus, by projections from regions of the PFC and other areas indicates that a more nuanced parcellation of its territories and variation in the distribution of neurons in these territories may help to elucidate variation in specific frontostriatal circuits contributing to the distinctive pathophysiology of select neurological disorders. For closely related disorders like WS and ASD, understanding variation in neuronal distribution in discrete functional territories may help to elucidate perturbations of neural circuitry in specific circuits and connectivity pathways, which will help to clarify the genetic and developmental mechanisms underlying these disorders.

**Acknowledgements** This research was supported in part by the National Institutes of Health grants P01 NICHD033113, 5R03MH103697, and 5T32MH020002. Human brain tissue was donated by families of individuals with Williams syndrome in partnership with the Williams Syndrome Association (Terry Monkaba, Executive Director), now maintained as part of the Ursula Bellugi Williams Syndrome Brain Collection, curated by KS at UCSD. Samples from neurotypical individuals were obtained in partnership with the University of Maryland Brain and Tissue Bank, a repository of the National Institutes of Health NeuroBioBank. We are grateful to individuals and their families who have participated in research efforts past and present to characterize the genetic, neuroanatomical, and behavioral features of Williams syndrome. We additionally thank Chelsea Brown, Valerie Judd, Hailee Orfant, Alexa Stephenson, Linnea Wilder, and Robert Miller for their technical assistance with tissue processing.

## Compliance with ethical standards

**Conflict of interest** The authors have no conflict of interest to declare.

## References

Adorjan I, Ahmed B, Feher V et al (2017) Calretinin interneuron density in the caudate nucleus is lower in autism spectrum disorder. Brain 140(7):2028–2040. https://doi.org/10.1093/brain/awx131

Atkinson J, Braddick O, Anker S et al (2003) Neurobiological models of visuospatial cognition in children with Williams syndrome: measures of dorsal-stream and frontal function. Dev Neuropsychol 23:139–172. https://doi.org/10.1080/87565641.2003.9651890

Atkinson J, Anker S, Braddick O et al (2007) Visual and visuospatial development in young children with Williams syndrome. Dev Med Child Neurol 43:330–337. https://doi.org/10.1111/j.1469-8749.2001.tb00213.x

Balsters JH, Mantini D, Wenderoth N (2017) Connectivity-based parcellation reveals distinct cortico-striatal connectivity fingerprints in Autism Spectrum Disorder. Neuroimage. https://doi.org/10.1016/j.neuroimage.2017.02.019

Barger N, Hanson KL, Teffer K et al (2014) Evidence for evolutionary specialization in human limbic structures. Front Hum Neurosci 8:277. https://doi.org/10.3389/fnhum.2014.00277

Berg JS, Brunetti-Pierri N, Peters SU et al (2007) Speech delay and autism spectrum behaviors are frequently associated with duplication of the 7q11.23 Williams-Beuren syndrome region. Genet Med 9:427–441. https://doi.org/10.1097/GIM.0b013e3180986192

Berke JD (2011) Functional properties of striatal fast-spiking interneurons. Front Syst Neurosci. https://doi.org/10.3389/fnsys.2011.00045

Bernácer J, Prensa L, Giménez-Amaya JM (2007) Cholinergic interneurons are differentially distributed in the human striatum. PLoS ONE. https://doi.org/10.1371/journal.pone.0001174

Bernácer J, Prensa L, Giménez-Amaya JM (2012) Distribution of GABAergic interneurons and dopaminergic cells in the functional territories of the human striatum. PLoS ONE. https://doi.org/10.1371/journal.pone.0030504

Bolam JP, Wainer BH, Smith AD (1984) Characterization of cholinergic neurons in the rat neostriatum. A combination of choline acetyltransferase immunocytochemistry, Golgi-impregnation and electron microscopy. Neuroscience 12:711–718. https://doi.org/10.1016/0306-4522(84)90165-9

Booth JR, Wood L, Lu D et al (2007) The role of the basal ganglia and cerebellum in language processing. Brain Res. https://doi.org/10.1016/j.brainres.2006.11.074

Brock J (2007) Language abilities in Williams syndrome: a critical review. Dev Psychopathol 19:97–127

Choi EY, Yeo BTT, Buckner RL (2012) The organization of the human striatum estimated by intrinsic functional connectivity. J Neurophysiol 108:2242–2263. https://doi.org/10.1152/jn.00270.2012

Contant C, Umbriaco D, Garcia S et al (1996) Ultrastructural characterization of the acetylcholine innervation in adult rat neostriatum. Neuroscience 71:937–947. https://doi.org/10.1016/0306-4522(95)00507-2

Craig LA, Hong NS, McDonald RJ (2011) Revisiting the cholinergic hypothesis in the development of Alzheimer's disease. Neurosci Biobehav Rev 35:1397–1409

Delmonte S, Gallagher L, O'Hanlon E et al (2013) Functional and structural connectivity of frontostriatal circuitry in Autism Spectrum Disorder. Front Hum Neurosci 7:430. https://doi.org/10.3389/fnhum.2013.00430

Estes A, Shaw D, Sparks B (2011) Basal ganglia morphometry and repetitive behavior in young children with autism spectrum disorder. Autism Research 4:212–220. https://doi.org/10.1002/aur.193

Fan CC, Brown TT, Bartsch H et al (2017) Williams syndrome-specific neuroanatomical profile and its associations with behavioral features. NeuroImage Clin 15:343–347. https://doi.org/10.1016/j.nicl.2017.05.011

Farran EK, Jarrold C (2003) Visuospatial cognition in Williams syndrome: reviewing and accounting for the strengths and weaknesses in performance. Dev Neuropsychol 23:173–200. https://doi.org/10.1080/87565641.2003.9651891

Gogolla N, Leblanc JJ, Quast KB et al (2009) Common circuit defect of excitatory-inhibitory balance in mouse models of autism. J Neurodev Disord 1:172–181. https://doi.org/10.1007/s11689-009-9023-x

Grahn JA, Parkinson JA, Owen AM (2008) The cognitive functions of the caudate nucleus. Prog Neurobiol 86:141–155. https://doi.org/10.1016/j.pneurobio.2008.09.004

Grahn JA, Da CC, Packard MG et al (2009) The role of the basal ganglia in learning and memory: neuropsychological studies. Behav Brain Res 199:53–60

Haber SN (2003) The primate basal ganglia: parallel and integrative networks. J Chem Neuroanat 26(4):317–330

Haber SN (2016) Corticostriatal circuitry. Dialogues Clin Neurosci 18:7–21

Haber SN, Behrens TEJ (2014) The neural network underlying incentive-based learning: implications for interpreting circuit disruptions in psychiatric disorders. Neuron 83:1019–1039

Haber SN, Knutson B (2010) The reward circuit: Linking primate anatomy and human imaging. Neuropsychopharmacology 35:4–26
Haber SN, Kim K-S, Mailly P, Calzavara R (2006) Reward-related cortical inputs define a large striatal region in primates that interface with associative cortical connections, providing a substrate for incentive-based learning. J Neurosci 26(32):8368–8376
Hanson KL, Cuevas DL, Groeniger KM et al (2018a) Decreased density of cholinergic interneurons in the medial caudate nucleus in humans with Williams syndrome. FASEB J. https://doi.org/10.1096/fasebj.2018.32.1_supplement.781.4
Hanson KL, Lew CH, Hrvoj-Mihic B et al (2018b) Increased glia density in the caudate nucleus in Williams syndrome: Implications for frontostriatal dysfunction in autism. Dev Neurobiol. https://doi.org/10.1002/dneu.22554
Hashemi E, Ariza J, Rogers H et al (2017) The number of parvalbumin-expressing interneurons is decreased in the medial prefrontal cortex in autism. Cereb Cortex. https://doi.org/10.1093/cercor/bhw021
Holt DJ, Graybiel ANNM, Saper CB (1997) Neurochemical architecture of the human striatum. J Comp Neurol 384:1–25
Holt DJ, Bachus SE, Hyde TM et al (2005) Reduced density of cholinergic interneurons in the ventral striatum in Schizophrenia: an in situ hybridization study. Biol Psychiatry 58:408–416. https://doi.org/10.1016/j.biopsych.2005.04.007
Hrvoj-Mihic B, Hanson KL, Lew CH et al (2017) Basal dendritic morphology of cortical pyramidal neurons in Williams syndrome: prefrontal cortex and beyond. Front Neurosci. https://doi.org/10.3389/fnins.2017.00419
Järvinen A, Korenberg JR, Bellugi U (2013) The social phenotype of Williams syndrome. Curr Opin Neurobiol 23:414–422
Järvinen-Pasley A, Bellugi U, Reilly J et al (2008) Defining the social phenotype in Williams syndrome: a model for linking gene, the brain, and behavior. Dev Psychopathol 20:1–35. https://doi.org/10.1017/S0954579408000011
Kalanithi PSA, Zheng W, Kataoka Y, DiFiglia M, Grantz H, Saper CB, Schwartz ML, Leckman JF, Vaccarino FM (2005) Altered parvalbumin-positive neuron distribution in basal ganglia of individuals with Tourette syndrome. Proc Nat Acad Sci 102(37):13307–13312
Karmiloff-Smith A, Grant J, Berthoud I et al (1997) Language and Williams syndrome: how intact is "intact"? Child Dev 68:246–262. https://doi.org/10.1111/j.1467-8624.1997.tb01938.x
Kataoka Y, Kalanithi PSA, Grantz H et al (2010) Decreased number of parvalbumin and cholinergic interneurons in the striatum of individuals with Tourette syndrome. J Comp Neurol 518:277–291. https://doi.org/10.1002/cne.22206
Kohls G, Schulte-Rüther M, Nehrkorn B et al (2013) Reward system dysfunction in autism spectrum disorders. Soc Cogn Affect Neurosci 8:565–572. https://doi.org/10.1093/scan/nss033
Koós T, Tepper JM (1999) Inhibitory control of neostriatal projection neurons by GABAergic interneurons. Nat Neurosci 2:467–472. https://doi.org/10.1038/8138
Langen M, Durston S, Staal WG et al (2007) Caudate nucleus is enlarged in high-functioning medication-naive subjects with autism. Biol Psychiatry 62:262–266. https://doi.org/10.1016/j.biopsych.2006.09.040
Langen M, Leemans A, Johnston P et al (2012) Fronto-striatal circuitry and inhibitory control in autism: findings from diffusion tensor imaging tractography. Cortex 48:183–193. https://doi.org/10.1016/j.cortex.2011.05.018
Lecumberri A, Lopez-Janeiro A, Corral-Domenge C, Bernacer J (2018) Neuronal density and proportion of interneurons in the associative, sensorimotor and limbic human striatum. Brain Struct Funct 4:1615–1625. https://doi.org/10.1007/s00429-017-1579-8
Lew CH, Brown C, Bellugi U, Semendeferi K (2017) Neuron density is decreased in the prefrontal cortex in Williams syndrome. Autism Res 10:99–112. https://doi.org/10.1002/aur.1677
Lew CH, Groeniger KM, Bellugi U et al (2018) A postmortem stereological study of the amygdala in Williams syndrome. Brain Struct Funct. https://doi.org/10.1007/s00429-017-1592-y
Lew CH, Groeniger KM, Hanson KL, Cuevas D, Greiner DMZ, Hrvoj-Mihic B, Bellugi U, Schumann CM, Semendeferi K (2020) Serotonergic innervation of the amygdala is increased in autism spectrum disorder and decreased in Williams syndrome. Mol Autism 11(1):12
Liégeois F, Baldeweg T, Connelly A et al (2003) Language fMRI abnormalities associated with FOXP2 gene mutation. Nat Neurosci 6:1230–1237. https://doi.org/10.1038/nn1138
Little K, Riby DM, Janes E et al (2013) Heterogeneity of social approach behaviour in Williams syndrome: the role of response inhibition. Res Dev Disabil 34:959–967. https://doi.org/10.1016/j.ridd.2012.11.020
Marín O (2012) Interneuron dysfunction in psychiatric disorders. Nat Rev Neurosci 13:107–120. https://doi.org/10.1038/nrn3155
Di Martino A, Kelly C, Grzadzinski R et al (2011) Aberrant striatal functional connectivity in children with autism. Biol Psychiatry 69:847–856. https://doi.org/10.1016/j.biopsych.2010.10.029
Martos YV, Braz BY, Beccaria JP, Murer MG, Belforte JE (2017) Compulsive social behavior emerges after selective ablation of striatal cholinergic interneurons. J Neurosci 11:2849–2858
Meyer-Lindenberg A, Kohn P, Mervis CB et al (2004) Neural basis of genetically determined visuospatial construction deficit in Williams syndrome. Neuron 43:623–631. https://doi.org/10.1016/j.neuron.2004.08.014
Mobbs D, Eckert MA, Mills D et al (2007) Frontostriatal dysfunction during response inhibition in Williams syndrome. Biol Psychiatry 62:256–261. https://doi.org/10.1016/j.biopsych.2006.05.041
Morris CA, Mervis CB (2000) Williams syndrome and related disorders. Annu Rev Genom Hum Genet 1:461–484. https://doi.org/10.1146/annurev.genom.1.1.461
Morris LS, Kundu P, Dowell N, Mechelmans DJ, Favre P, Irvine MA, Robbins TW, Daw N, Bullmore ET, Harrison NA, Voon V (2016) Fronto-striatal organization: defining functional and microstructural substrates of behavioural flexibility. Cortex 74:118–133
Nakamura M, Watanabe K, Matsumoto A et al (2001) Williams syndrome and deficiency in visuospatial recognition. Dev Med Child Neurol 43:617–621. https://doi.org/10.1017/S0012162201001128
Nakano K, Kayahara T, Tsutsumi T, Ushiro H (2000) Neural circuits and functional organization of the striatum. J Neurol 247:V1–V15. https://doi.org/10.1007/PL00007778
Nava-Mesa MO, Jiménez-Díaz L, Yajeya J, Navarro-Lopez JD (2014) GABAergic neurotransmission and new strategies of neuromodulation to compensate synaptic dysfunction in early stages of Alzheimer's disease. Front Cell Neurosci 8:167
Nelson SB, Valakh V (2015) Excitatory/inhibitory balance and circuit homeostasis in autism spectrum disorders. Neuron 87:684–698
Pakhotin P, Bracci E (2007) Cholinergic interneurons control the excitatory input to the striatum. J Neurosci 27:391–400. https://doi.org/10.1523/jneurosci.3709-06.2007**(27/2/391 [pii]\r)**
Peñagarikano O, Abrahams BS, Herman EI et al (2011) Absence of CNTNAP2 leads to epilepsy, neuronal migration abnormalities, and core autism-related deficits. Cell. https://doi.org/10.1016/j.cell.2011.08.040
Perez-Costas E, Melendez-Ferro M, Roberts RC (2010) Basal ganglia pathology in schizophrenia: dopamine connections and anomalies. J Neurochem 113:287–302
Phillips CE, Jarrold C, Baddeley AD et al (2004) Comprehension of Spatial language terms in Williams syndrome: evidence for an

interaction between domains of strength and weakness. Cortex 40:85–101. https://doi.org/10.1016/S0010-9452(08)70922-5
Pober BR (2010) Williams–Beuren syndrome. N Engl J Med 362:239–252. https://doi.org/10.1056/NEJMra0903074
Prensa L, Giménez-Amaya JM, Parent A (1999) Chemical heterogeneity of the striosomal compartment in the human striatum. J Comp Neurol 413(4):603–618. https://doi.org/10.1002/(SICI)1096-9861(19991101)413:4%3C603::AID-CNE9%3E3.0.CO;2-K
Raghanti MA, Stimpson CD, Marcinkiewicz JL et al (2008) Cholinergic innervation of the frontal cortex : differences among humans, chimpanzees, and macaque monkeys. Comp Gen Pharmacol 424:409–424. https://doi.org/10.1002/cne
Raghanti MA, Edler MK, Stephenson AR et al (2016) Human-specific increase of dopaminergic innervation in a striatal region associated with speech and language: a comparative analysis of the primate basal ganglia. J Comp Neurol 524:2117–2129. https://doi.org/10.1002/cne.23937
Rapanelli M, Frick LR, Pittenger C (2017) The role of interneurons in autism and Tourette syndrome. Trends Neurosci 40(7):397–407
Reiss AL, Eliez S, Schmitt JE et al (2000) Neuroanatomy of Williams syndrome: a high-resolution MRI study. J Cogn Neurosci 12(Suppl 1):65–73. https://doi.org/10.1162/089892900561986
Reiss AL, Eckert MA, Rose FE et al (2004) An experiment of nature: brain anatomy parallels cognition and behavior in Williams syndrome. J Neurosci 24:5009–5015. https://doi.org/10.1523/jneurosci.5272-03.2004
Robinson BF, Mervis CB, Robinson BW (2003) The roles of verbal short-term memory and working memory in the acquisition of grammar by children with Williams syndrome. Dev Neuropsychol 23:13–31. https://doi.org/10.1080/87565641.2003.9651885
Rodgers J, Riby DM, Janes E et al (2012) Anxiety and repetitive behaviours in autism spectrum disorders and Williams syndrome: a cross-syndrome comparison. J Autism Dev Disord. https://doi.org/10.1007/s10803-011-1225-x
Sampaio A, Sousa N, Férnandez M et al (2008) Memory abilities in Williams syndrome: dissociation or developmental delay hypothesis? Brain Cogn 66:290–297. https://doi.org/10.1016/j.bandc.2007.09.005
Sampaio A, Sousa N, Férnandez M et al (2010) Williams syndrome and memory: a neuroanatomic and cognitive approach. J Autism Dev Disord 40:870–877. https://doi.org/10.1007/s10803-010-0940-z
Sanabria-Castro A, Alvarado-Echeverría I, Monge-Bonilla C (2017) Molecular pathogenesis of alzheimer's disease: an update. Ann Neurosci 24:46–54
Sanders SJ, Murtha MT, Gupta AR et al (2012) De novo mutations revealed by whole-exome sequencing are strongly associated with autism. Nature 485:237–241. https://doi.org/10.1038/nature10945
Schumann CM, Amaral DG (2006) Stereological analysis of amygdala neuron number in autism. J Neurosci 26:7674–7679. https://doi.org/10.1523/jneurosci.1285-06.2006
Searcy YM, Lincoln AJ, Rose FE et al (2004) The relationship between age and IQ in adults with Williams syndrome. Am J Ment Retard 109:231–236. https://doi.org/10.1352/0895-8017(2004)109%3c231:TRBAAI%3e2.0.CO;2
Sears LL, Vest C, Mohamed S et al (1999) An MRI study of the basal ganglia in autism. Prog Neuro-Psychopharmacol Biol Psychiatry 23:613–624. https://doi.org/10.1016/S0278-5846(99)00020-2
Selden N, Geula C, Hersh L, Mesulam MM (1994a) Human striatum: chemoarchitecture of the caudate nucleus, putamen and ventral striatum in health and Alzheimer's disease. Neuroscience 60:621–636. https://doi.org/10.1016/0306-4522(94)90491-X
Selden N, Mesulam MM, Geula C (1994b) Human striatum: the distribution of neurofibrillary tangles in Alzheimer's disease. Brain Res 648:327–331. https://doi.org/10.1016/0006-8993(94)91136-3
Shafritz KM, Dichter GS, Baranek GT, Belger A (2008) The neural circuitry mediating shifts in behavioral response and cognitive set in autism. Biol Psychiatry 63:974–980. https://doi.org/10.1016/j.biopsych.2007.06.028
Sherwood CC, Raghanti MA, Stimpson CD, Spocter MA, Uddin M, Boddy AM, Wildman DE, Bonar CJ, Lewandowski AH, Phillips KA, Erwin JM, Hof PR (2009) Inhibitory interneurons of the human prefrontal cortex display conserved evolution of the phenotype and related genes. Proc Royal Soc B Biol Sci 277(1684):1011–1020
Stephenson AR, Edler MK, Erwin JM et al (2017) Cholinergic innervation of the basal ganglia in humans and other anthropoid primates. J Comp Neurol 525:319–332. https://doi.org/10.1002/cne.24067
Tepper JM, Tecuapetla F, Koós T, Ibáñez-Sandoval O (2010) Heterogeneity and diversity of striatal GABAergic interneurons. Front Neuroanat. https://doi.org/10.3389/fnana.2010.00150
Vargha-Khadem F, Watkins KE, Price CJ et al (1998) Neural basis of an inherited speech and language disorder. Proc Natl Acad Sci U S A 95:12695–12700. https://doi.org/10.1073/pnas.95.21.12695
Velleman SL, Mervis CB (2011) Children with 7q11.23 duplication syndrome: speech, language, cognitive, and behavioral characteristics and their implications for intervention. Perspect Lang Learn Educ 18:108–116. https://doi.org/10.1044/lle18.3.108
Viñas-Guasch N, Wu YJ (2017) The role of the putamen in language: a meta-analytic connectivity modeling study. Brain Struct Funct. https://doi.org/10.1007/s00429-017-1450-y
Wegiel J, Flory M, Kuchna I et al (2014) Stereological study of the neuronal number and volume of 38 brain subdivisions of subjects diagnosed with autism reveals significant alterations restricted to the striatum, amygdala and cerebellum. Acta Neuropathol Commun 2:141. https://doi.org/10.1186/s40478-014-0141-7
Wilder L, Hanson KL, Lew CH et al (2018) Decreased neuron density and increased glia density in the ventromedial prefrontal cortex (Brodmann area 25) in Williams syndrome. Brain Sci. https://doi.org/10.3390/brainsci8120209
Wu Y, Parent A (2000) Striatal interneurons expressing calretinin, parvalbumin or NADPH-diaphorase: a comparative study in the rat, monkey and human. Brain Res 863:182–191. https://doi.org/10.1016/S0006-8993(00)02135-1
Yizhar O, Fenno LE, Prigge M et al (2011) Neocortical excitation/inhibition balance in information processing and social dysfunction. Nature 477:171–178. https://doi.org/10.1038/nature10360
Zikopoulos B, Barbas H (2013) Altered neural connectivity in excitatory and inhibitory cortical circuits in autism. Front Hum Neurosci 7:609. https://doi.org/10.3389/fnhum.2013.00609